

Rapid sympathetic cooling to Fermi degeneracy on a chip

S. Aubin, S. Myrskog, M.H.T. Extavour, L.J. LeBlanc, D. McKay, A. Stummer, J.H. Thywissen
Department of Physics, University of Toronto, Toronto, Ontario M5S 1A7, CANADA

(Dated: February 19, 2019)

Quantum degenerate gases of neutral fermions present new opportunities for testing many-body condensed matter systems, realizing precision atom interferometry, producing ultra-cold molecules, and investigating fundamental forces. Since their first observation [1], degenerate Fermi gases (DFGs) have continued to be challenging to produce, and have been realized in only a handful of laboratories [2, 3, 4, 5, 6, 7, 8, 9, 10]. In this Letter we report the production of a DFG achieved using a simple apparatus based on a microfabricated electromagnetic (μ EM) trap. Similar approaches applied to Bose-Einstein Condensation (BEC) of ^{87}Rb [11, 12] have accelerated evaporative cooling and eliminated the need for multiple vacuum chambers. We demonstrate sympathetic cooling for the first time in a μ EM trap, and cool ^{40}K to Fermi degeneracy in just six seconds — five to ten times faster than has been possible in conventional magnetic traps. To understand our sympathetic cooling trajectory, we measure the temperature dependence of the ^{40}K - ^{87}Rb cross-section and observe its Ramsauer-Townsend reduction.

Microfabricating the electromagnets used to trap ultracold atoms leads to a series of experimental benefits. Decreasing the radius R of a surface-mounted wire increases the maximum magnetic field gradient as $R^{-1/2}$ [13]. Since the oscillation frequency ω of the trapped atoms increases linearly with transverse field gradient, decreasing R from centimeters to micrometers can increase confinement frequency by orders of magnitude. In addition, one can envision a “lab on a chip,” in which multiple devices are integrated on a single device, expediting applications for complex manipulation of fermionic atoms for simulations of strongly correlated systems [14], quantum transport experiments [15], and precision interferometry [16]. The strong confinement provided by a μ EM trap on a chip also has a practical advantage: it facilitates faster cooling, which relaxes constraints on vacuum quality and leads to a tremendous simplification over traditional DFG experiments that require multiple ovens, Zeeman slowers, or two magneto-optical traps (MOTs).

In our system [17], the entire experimental cycle takes place in a single vapour cell (Fig. 1a). Counter-propagating laser beams collect, cool, and trap 2×10^7 ^{40}K and 10^9 ^{87}Rb atoms in a MOT. Atoms are transferred to a purely magnetic trap formed by external quadrupole coils and transported to the chip 5 cm away. Figure 1b shows several microscopic gold wires supported

by the substrate. In the presence of uniform magnetic fields, current flow through the central ‘Z’-shaped wire creates a magnetic field minimum 200 μm from the surface of the chip. At the centre of this trap, the ^{40}K radial (longitudinal) oscillation frequency is $\omega_\perp/2\pi = 823 \pm 7$ Hz ($\omega_\ell/2\pi = 46.2 \pm 0.7$ Hz). The corresponding ^{87}Rb trap frequencies are a factor of $\sqrt{m_{\text{Rb}}/m_K} \approx 1.47$ smaller, where m_{Rb} and m_K are the atomic masses of ^{87}Rb and ^{40}K , respectively.

After loading, the 1.1-mK-deep chip trap holds approximately 2×10^5 ^{40}K and 2×10^7 ^{87}Rb doubly spin-polarized atoms, at a temperature $\gtrsim 300$ μK . Lower temperatures are achieved by forced evaporative cooling of ^{87}Rb . A field oscillating at RF frequency ν_{RF} (typically swept from 30 MHz to 3.61 MHz) selectively removes the highest energy ^{87}Rb atoms by driving spin-flip transitions to untrapped states.

The ^{40}K atoms, with smaller Zeeman splittings, are not ejected but are sympathetically cooled [2, 18, 19] by thermalizing with the ^{87}Rb reservoir via ^{40}K - ^{87}Rb collisions [6, 8, 9, 23].

The evolution of temperature T and atom number N during sympathetic cooling is measured by releasing atoms from the trap and observing their expansion with absorptive imaging. Figure 2 shows the cooling of ^{40}K and ^{87}Rb to dual quantum degeneracy. Due to the tight confinement of the μ EM trap, this 10^{12} increase in Fermi degeneracy takes only 6 s. The steep ascent of ^{40}K to quantum degeneracy also demonstrates the efficiency of sympathetic cooling. Since ^{40}K is a rare isotope and therefore more difficult to collect from vapour than ^{87}Rb , this inherent efficiency is a significant advantage over direct evaporation. To our knowledge, this is the first observation of sympathetic cooling, of Fermi degeneracy, and of dual degeneracy in a μ EM trap.

Below $T \approx 1$ μK , we observe two independent signatures of Fermi degeneracy. We measure the ^{40}K release energy by fitting the density profile to a Gaussian with rms radius r_K . Figure 3 shows the release energy (proportional to r_K^2) versus temperature, in comparison to both the classical (Boltzmann) and the quantum (Fermi) expectations. We observe that though the gas is non-interacting, it approaches a finite release energy at zero temperature. The observed “Pauli pressure” is a signature of Fermi statistics [2]: at zero temperature, fermions fill all available states up to the Fermi energy $E_F = \hbar(6N\omega_\perp^2\omega_\ell)^{1/3}$, where N is the number of fermions. A second signature of Fermi statistics is evident in the shape of the cloud. Figure 3c compares the residuals of a Gaussian fit (which assumes Boltzmann statistics) and a polylogarithmic fit (which assumes Fermi statistics).

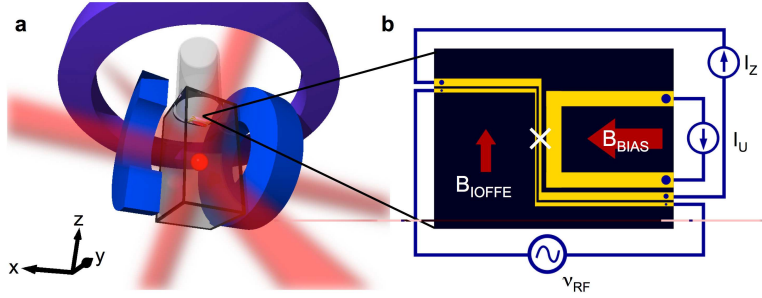


FIG. 1: **A simple apparatus for Fermi degeneracy.** (a) The dual-species MOT (red sphere) is formed at the intersection of six laser beams. The cloud is then magnetically trapped using external quadrupole coils (blue), transported 5 cm vertically using an offset coil (purple), and compressed in the μ EM trap. (b) Schematic diagram of the central region of the μ EM chip. A magnetic trap is formed at the location marked with a white “X” by applying $I_Z = 2.0$ A, $I_U = 30$ mA, $B_{BIAS} = 21.4$ G, and $B_{IOFFE} = 5.2$ G. Wire widths from left to right are 20 μ m, 60 μ m, and 420 μ m.

The Fermi distribution describes the data well, with a χ^2 three times lower than the Gaussian fit. After all ^{87}Rb atoms have been evaporated, we use polylog fits to measure temperature, and find $k_B T / E_F$ as low as 0.09 ± 0.05 with as many as 4×10^4 ^{40}K atoms.

We empirically optimize the sympathetic cooling trajectory, and find that RF sweep times faster than 6 s are not successful, whereas ^{87}Rb alone can be cooled to degeneracy in 2 s. This indicates that ^{40}K and ^{87}Rb rethermalize more slowly than ^{87}Rb with itself. Measuring the temperature ratio during sympathetic cooling (Fig. 4a) reveals that ^{40}K lags behind ^{87}Rb at high temperatures, despite the fact that our optimal frequency ramp starts slowly (when the atoms are hottest), and accelerates at lower temperatures.

In the low-temperature limit, we do not expect the cross-species thermalization to lag the ^{87}Rb - ^{87}Rb ther-

malization, since the ^{40}K - ^{87}Rb cross-section $\sigma_{\text{KRb}} = 1520(83)$ nm 2 [20] exceeds the ^{87}Rb - ^{87}Rb cross-section, $\sigma_{\text{RbRb}} = 689.6(3)$ nm 2 [21]. However, several conflicting values for σ_{KRb} have been recently presented [20, 22, 23].

To investigate σ_{KRb} further, we measure the cross-species thermalization rate [24] at several temperatures. Starting from equilibrium, we abruptly reduce ν_{RF} , wait for a variable hold time to allow cross-thermalization, and then measure the ^{40}K temperature, as shown in Fig. 4b. We repeat this measurement at several temperatures, and fit each to the model of Ref. [25]. We find that the cross-section has a dramatic dependence on temperature, decreasing by an order of magnitude between 10 μK and 70 μK (see fig. 4c).

The interaction between atoms can often be approximated by a delta-function contact potential. Fig. 4c shows that the s-wave scattering cross-section of this “naive” model (further described in Methods) would predict a higher σ_{KRb} than σ_{RbRb} throughout our cooling cycle. By contrast, our data show a σ_{KRb} smaller than σ_{RbRb} above 30 μK . This trend is reproduced by an effective range model [26], which includes a reduction in scattering phase (and thus cross-section) below the naive expectation. The observed reduction in scattering cross-section is due to the Ramsauer-Townsend effect, in which the s-wave scattering phase and cross-section approach zero for a particular value of relative energies between particles [27].

Extrapolating these results to the temperature at which we begin sympathetic cooling (~ 300 μK), the thermally averaged ^{40}K - ^{87}Rb cross-section is reduced below the ^{87}Rb - ^{87}Rb cross-section, explaining the requirement for a slow initial RF frequency sweep for sympathetic cooling. Below 15 μK , where no temperature lag is observed, σ_{KRb} exceeds σ_{RbRb} .

In conclusion, we have achieved simultaneous quantum degeneracy of bosonic and fermionic atoms in a μ EM trap and demonstrated an approach that may simplify future research in Fermi systems. We have measured the temperature dependent ^{40}K - ^{87}Rb cross-section and observe a sharp decrease at temperatures above 50 μK .

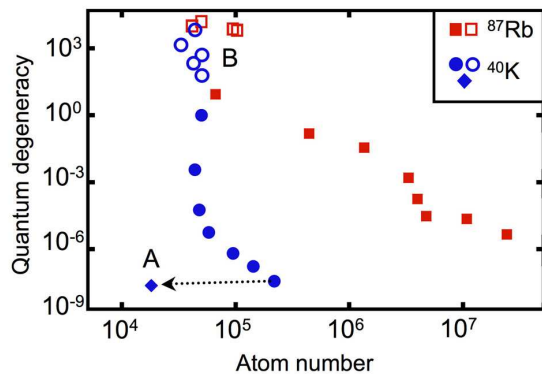


FIG. 2: **Sympathetic cooling in a chip trap.** Spin-polarized fermions without a bosonic bath cannot be successfully evaporated (A). However, if bosonic ^{87}Rb is evaporatively cooled, then fermionic ^{40}K is sympathetically cooled to quantum degeneracy (B). The vertical axis is phase space density (filled symbols) up to a maximum value of 1, above which (open symbols) the fugacity is plotted for fermions and ground state occupation (number of atoms in the condensate) is plotted for bosons.

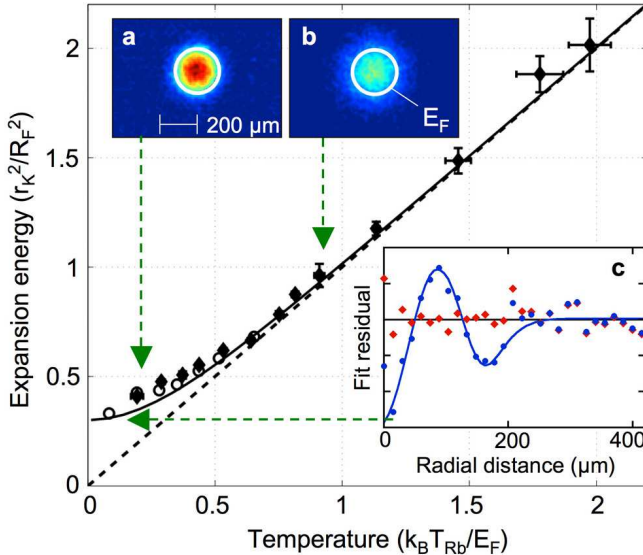


FIG. 3: Observation of Fermi statistics. The quantity r_K^2 is proportional to expansion energy, and is plotted versus the temperature of the ^{87}Rb reservoir. The vertical axis is scaled using $R_F^2 = E_F(\omega_{\perp}^{-2} + t^2)/m_K$, where t is the expansion time before imaging. The temperature is also scaled by the Fermi energy E_F (typically $k_B \times 1.1 \mu\text{K}$) of each ^{40}K cloud. Gaussian fits of data taken with both thermal (diamonds) and Bose-condensed (circles) ^{87}Rb is compared a Gaussian fit of an ideal Fermi distribution (solid line) and its classical expectation (dashed line). Absorption images are shown for $k_B T/E_F = 0.95$ (a) and 0.35 (b), including a white circle indicating the Fermi energy E_F . (c) The fit residuals of a radially averaged cloud profile show a strong systematic deviation when assuming Boltzmann (blue circles) instead of Fermi (red diamonds) statistics. A degenerate Fermi cloud is flatter at its centre than a Boltzmann distribution, and falls more sharply to zero near its edge.

This Ramsauer-Townsend effect is an important consideration when optimizing sympathetic cooling in similar systems. The high trap frequency provided by μEM traps enables us to attain quantum degeneracy of fermions five to ten times faster than typical with conventional traps [1, 2, 3, 4, 5, 6, 7, 8, 9, 10]. Tight confinement also boosts the ratio of Fermi energy E_F to the recoil energy $\hbar^2 k^2/2m_K$. The ratio reported here is ~ 2.5 , one of the highest reported to date, and within the regime required to observe Pauli blocking of light scattering off degenerate fermions [29, 30].

Methods

Loading. Our experimental cycle is similar to that described in Ref. [17], with several key modifications emphasized here and in the main text. Approximately 600 mW of incoherent 405 nm light desorbs atoms from the pyrex vacuum cell walls, boosting the MOT atom number one hundred-fold compared to loading from the

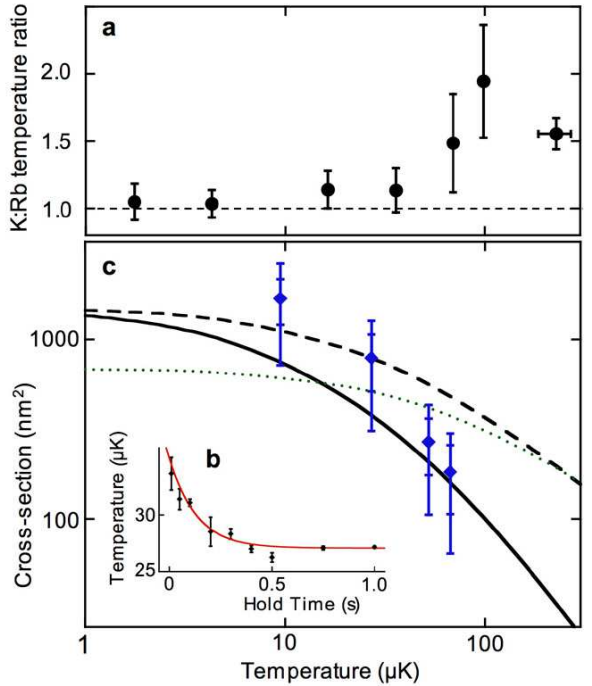


FIG. 4: Cross-species thermalization. (a) The ratio of the temperature of ^{40}K to the temperature of ^{87}Rb approaches unity as temperature is lowered during sympathetic cooling. (b) We measure cross-thermalization by abruptly reducing the temperature of ^{87}Rb and watching the temperature of ^{40}K relax versus time. The data shown has an asymptotic ^{40}K temperature of $27 \mu\text{K}$. (c) Measurements of σ_{KRb} (points) are compared to the ‘naive’ model (dashed) and an effective range model (solid), both described in the text. Two sets of error bars are shown: the smaller set include only statistical error, and the larger set include a systematic uncertainty in atom number. For reference, the s-wave σ_{RbRb} is also shown (dotted).

background vapour [17]. Potassium alone is first loaded into the MOT for 25 s, after which ^{87}Rb is loaded for an additional 3-5 s, while maintaining the ^{40}K population. Both MOTs operate with a detuning of -26 MHz , until the last 10 ms, when ^{40}K is compressed with a -5 MHz detuning. After MOT loading, 3 ms of optical molasses cooling is applied to the ^{87}Rb atoms, while the ^{40}K atoms are optically pumped into the $|F = 9/2, m_F = 9/2\rangle$ hyperfine ground state.

Chip. Two defects are present near the centre of the principal Z-wire, which result in the formation of three ‘dimples’ in the trapping potential. We use the magnetic gradient generated by 30 mA of current through the U-wire to centre the magnetic trap on one of these dimples.

Fermi fits. Degenerate Fermi clouds are fit to $Af_2(\mathcal{Z} \exp[-\varrho^2/2r^2])$, where ϱ is the radial coordinate, $Af_2(\mathcal{Z})$ is the peak optical density, \mathcal{Z} the fugacity, and $f_\nu(q) = -\sum_{\ell=1}^{\infty} (-q)^\ell/\ell^\nu$ is the polylogarithmic function. The temperature is given by $k_B T = r^2 m_K / (\omega_{\perp}^{-2} + t^2)$, where r is the fit width and t the time of flight. Atom

number is extracted using $N = 2\pi r^2 f_3(\mathcal{Z})A/\sigma_\lambda$, where σ_λ is the resonant absorption cross-section. T/T_F can be extracted directly from the fugacity using $(T/T_F)^{-3} = 6f_3(\mathcal{Z})$. Non-degenerate clouds are fit to a Gaussian distribution of positions, with the same interpretation of r . Systematic uncertainty in temperature measurement are estimated at $\pm 20\%$ by comparing measurements along orthogonal imaging axes.

Thermalization. When the ^{87}Rb atom number N_{Rb} is much larger than the ^{40}K atom number, the relaxation of the ^{40}K temperature T to T_{final} is described by $\dot{u} = -u\tau^{-1}(1 + m_{\text{Rb}}u/(m_{\text{Rb}} + m_{\text{K}}))^{\frac{1}{2}}(1 + u/2)^{-\frac{3}{2}}$, where $u \equiv (T/T_{\text{final}}) - 1$, and thermalization time τ given by

$$\frac{1}{\tau} = \frac{\sqrt{2}}{3\pi^2} \frac{\sigma_{\text{KRB}}}{k_{\text{B}}T_{\text{final}}} \frac{\sqrt{m_{\text{K}}}m_{\text{Rb}}^2\omega_\perp^2\omega_\ell}{(m_{\text{K}} + m_{\text{Rb}})^{3/2}} N_{\text{Rb}}, \quad (1)$$

in which trap frequencies are for ^{87}Rb [25]. Fitting for τ

allows us to extract σ_{KRB} . Note that all thermalization data is taken with N_{K} below 4% of N_{Rb} .

Theory. The “naive” interaction model discussed in the text gives $\sigma_{\text{KRB}} = 4\pi a^2/(1 + a^2k^2)$, where a is the s-wave scattering length and k is the relative wave vector in the centre of mass frame. Fig. 4c shows the thermally averaged cross-section.

Scattering length. The precision of the extracted cross-sections is not sufficient to improve current estimates of the ^{40}K - ^{87}Rb scattering length. Using the effective range theory to fit our measured cross-sections, we find $a_{\text{KRB}} = -16.5 \pm 2.6 \text{ nm}$, where the uncertainty is statistical. A factor of 1.5 underestimate of our atom number would bring this measured scattering length in agreement with the most recent values [20].

[1] DeMarco, B. & Jin, D. S., Onset of Fermi degeneracy in a trapped atomic gas. *Science* **285**, 1703 (1999).

[2] Truscott, A. G., Strecker, K. E., McAlexander, W. I., Partridge, G. B., & Hulet, R. G. Observation of Fermi pressure in a gas of trapped atoms. *Science* **291**, 2570 (2001).

[3] Schreck, F., *et al.* Quasipure Bose-Einstein condensate immersed in a Fermi sea. *Phys. Rev. Lett.* **87**, 080403 (2001).

[4] Granade, S. R., Gehm, M. E., O’Hara, K. M., & Thomas, J. E. Preparation of a degenerate, two-component fermi gas by evaporation in a single beam optical trap. *Phys. Rev. Lett.* **88**, 120405 (2002).

[5] Hadzibabic, Z., *et al.* Two-Species Mixture of Quantum Degenerate Bose and Fermi Gases. *Phys. Rev. Lett.* **88**, 160401 (2002).

[6] Roati, G., Riboli, F., Modugno, G., & Inguscio, M. Fermi-Bose quantum degenerate ^{40}K - ^{87}Rb mixture with attractive interaction. *Phys. Rev. Lett.* **89**, 150403 (2002).

[7] Bartenstein, M., *et al.* Crossover from a Molecular Bose-Einstein Condensate to a Degenerate Fermi Gas. *Phys. Rev. Lett.* **92**, 120401 (2004).

[8] Köhl, M., Moritz, H., Stöferle, T., Günter, K., & Esslinger T. Fermionic Atoms in a Three Dimensional Optical Lattice: Observing Fermi Surfaces, Dynamics, and Interactions. *Phys. Rev. Lett.* **94**, 080403 (2005).

[9] Ospelkaus, C., Ospelkaus, S., Sengstock, K., & Bongs, K. Interaction-driven dynamics of ^{40}K - ^{87}Rb Fermi-Bose gas mixtures in the large particle number limit. arXiv:cond-mat/0507219 (2005).

[10] Silber, C., *et al.* Quantum-degenerate mixture of fermionic lithium and bosonic rubidium gases. *Phys. Rev. Lett.* **95**, 170408 (2005).

[11] Hänsel, W., Hommelhoff, P., Hänsch, T. W., & Reichel, J., Bose-Einstein condensation on a microelectronic chip. *Nature* **413**, 498 (2001).

[12] Ott, H., Fortagh, J., Schlotterbeck, G., Grossmann, A., & Zimmermann, C. Bose-Einstein condensation in a surface microtrap. *Phys. Rev. Lett.* **87**, 230401 (2001).

[13] Groth, S., *et al.* Atom chips: Fabrication and thermal properties. *App. Phys. Lett.*, **85**, 2980 (2004).

[14] Hofstetter, W., Cirac, J. I., Zoller, P., Demler, E., & Lukin, M. D. High-temperature superfluidity of fermionic atoms in optical lattices. *Phys. Rev. Lett.*, **89**, 220407 (2002).

[15] Thywissen, J. H., Westervelt, R. M., & Prentiss, M., Quantum Point Contacts for Neutral Atoms. *Phys. Rev. Lett.* **83**, 3762 (1999).

[16] Wang Y.-J., *et al.* Atom Michelson Interferometer on a Chip Using a Bose-Einstein Condensate. *Phys. Rev. Lett.* **94**, 090405 (2005).

[17] Aubin, S., *et al.* Trapping fermionic ^{40}K and bosonic ^{87}Rb in a chip trap. *J. Low Temp. Phys.* **140**, 377 (2005).

[18] Myatt, C. J., Burt, E. A., Ghrist, R. W., Cornell, E. A., & Wieman, C. E. Production of Two Overlapping Bose-Einstein Condensates by Sympathetic Cooling. *Phys. Rev. Lett.* **78**, 586 (1997).

[19] Schreck, F., *et al.* Sympathetic cooling of bosonic and fermionic lithium gases towards quantum degeneracy. *Phys. Rev. A* **64**, 011402 (2001).

[20] Ferliano, F., *et al.* Precise determination of K-Rb scattering lengths from Feshbach spectroscopy. arXiv:cond-mat/0510630 (2005).

[21] van Kempen, E. G. M., Kokkelmans, S. J. J. M. F. Heinzen, J. J., & Verhaar, B. J. Interisotope determination of ultracold rubidium interactions from three high-precision experiments. *Phys. Rev. Lett.* **88**, 93201 (2002).

[22] Modugno, G., *et al.* Collapse of a Degenerate Fermi Gas. *Science* **297**, 2240 (2002).

[23] Goldwin, J., *et al.* Measurement of the interaction strength in a Bose-Fermi mixture with ^{87}Rb and ^{40}K . *Phys. Rev. A* **70**, 021601 (2004).

[24] Anderlini, M., *et al.* Sympathetic cooling and collisional properties of a Rb-Cs mixture. *Phys. Rev. A* **71**, 061401 (2005).

[25] Mosk, A., *et al.* Mixture of ultracold lithium and cesium atoms in an optical dipole trap. *Appl. Phys. B* **73**, 791 (2001).

[26] Flambaum, V. V., Gribakin, G. F., & Harabati, C. Ana-

lytical calculation of cold-atom scattering. *Phys. Rev. A* **59**, 1998 (1999).

[27] Townsend, J. S., *A Modern Approach to Quantum Mechanics* (New York: McGraw-Hill, 1992) p. 393, and references therein.

[28] Andrea Simoni, private communication.

[29] Busch, Th., Anglin, J. R., Cirac, J. I., & Zoller, P. Inhibition of spontaneous emission in Fermi gases. *Europhys. Lett.* **44** 1 (1998).

[30] DeMarco, B. & Jin, D. S. Exploring a quantum degenerate gas of fermionic atoms. *Phys. Rev. A* **58** R4267 (1998).

Acknowledgments: We would like to thank D. Jin, J.

Dalibard, J. Bohm, and D. Guery-Odelin for conversations about scattering theory. We also thank N. Bigelow, A. Aspect, and T. Schumm for stimulating conversations, P. Bouyer and R. Nyman for providing a tapered amplifier used in this work, and J. Estève for fabricating the chip used in this work. This work is supported by the NSERC, CFI, OIT, PRO, CRC, and Research Corporation. S.A., L.J.L. and D.M. acknowledge support from NSERC. M.H.T.E. acknowledges support from OGS. **Competing financial interests:** The authors declare that they have no competing financial interests.